tive for OKT1 and positive for OKT3) and by their differing patterns of reactivity with T cell lines. The binding pattern of OKT4 was quite distinct from OKT1 and OKT3; OKT4 bound only 55 percent of peripheral T cells and 80 percent of thymocytes. Furthermore, the pattern of binding of OKT4 to T cell lines was distinct from that of OKT1 and OKT3. Detailed studies demonstrated that OKT1, OKT3, and OKT4 were all nonreactive with peripheral B cells, monocytes, granulocytes, null cells, and B cell lines (*9*).

We have previously shown that the OKT1$^+$ population of peripheral lymphocytes are indeed the cells responsible for the T cell functions of mitogen reactivity, mixed lymphocyte culture responsivity, and proliferate response to soluble antigens. Furthermore we have shown that OKT1 defines a minor population of thymocytes responding in mixed lymphocyte culture but lacking mitogen responsivity (*9*). Preliminary studies suggest that OKT4$^+$ peripheral cells contain the helper T cell population.

Our present studies demonstrate the generation of monoclonal antibodies identifying antigens restricted to functional subclasses of T cells. Although our procedures entailed immunizing mice with the entire range of antigens represented on human T cells, we were able to retrieve hybrid cells producing monoclonal antibody reacting selectively with T cell subpopulations. Such antibodies should be invaluable for both diagnosis (*10*) and therapy (*11*) in clinical medicine.

PATRICK C. KUNG
GIDEON GOLDSTEIN
Ortho Pharmaceutical Corporation, Raritan, New Jersey 08869
ELLIS L. REINHERZ
STUART F. SCHLOSSMAN
Division of Tumor Immunology, Sidney Farber Cancer Institute, Harvard Medical School, Boston, Massachusetts 02115

References and Notes

1. H. Cantor and E. A. Boyse, *Cold Spring Harbor Symp. Quant. Biol.* **41**, 23 (1977); L. Chess and S. F. Schlossman, *Contemp. Top. Immunobiol.* **7**, 363 (1977); E. L. Reinherz and S. F. Schlossman, *J. Immunol.* **122**, 1335 (1979).
1a. R. L. Evans, H. Lazarus, A. C. Penta, S. F. Schlossman, *J. Immunol.* **129**, 1423 (1978).
2. A. J. Strelkauskas, V. Schauf, B. S. Wilson, L. Chess, S. F. Schlossman, *ibid.* **120**, 1278 (1978); L. Moretta, M. Ferrarini, A. Mingari, A. Moretta, S. R. Webb, *ibid.* **117**, 2171 (1976); J. H. Wybran and H. H. Fudenberg, *Trans. Assoc. Am. Phys.* **84**, 239 (1971).
3. G. Kohler and C. Milstein, *Nature (London)* **256**, 495 (1975).
4. C. J. Barnstable, W. F. Bodmer, G. Brown, G. Galfa, C. Milstein, A. F. Williams, *Cell* **14**, 9 (1978); M. M. Trucco, J. W. Stocker, R. Ceppellini, *Nature (London)* **273**, 666 (1978); H. Koprowski, Z. Steplewski, D. Herlyn, M. Herlyn, *Proc. Natl. Acad. Sci. U.S.A.* **71**, 3405 (1978).
5. Abbreviations: PBS, phosphate-buffered saline; DMA, Dulbecco modified minimum essential medium; PEG, polyethylene glycol; IFS, heat-inactivated fetal calf serum; IHS, heat-inactivated horse serum; DMSO, dimethyl sulfoxide; and HAT, hypoxanthine, aminopterin, and thymidine.
6. N. F. Mendes, M. C. A. Tolnai, N. P. A. Silveira, R. B. Gilbertson, R. S. Mitzgar, *J. Immunol.* **111**, 860 (1973).
7. R. Levy and J. Dilley, *ibid.* **119**, 394 (1977).
8. R. Levy, J. Dilley, L. A. Lampson, *Cur. Top. Microbiol. Immunol.* **81**, 164 (1978).
9. E. L. Reinherz, P. C. Kung, G. Goldstein, S. F. Schlossman, *J. Immunol.* **123**, 1233 (1979); *Proc. Natl. Acad. Sci. U.S.A.* **76**, 4061 (1979).
10. E. L. Reinherz, L. M. Nadler, D. S. Rosenthal, W. C. Moloney, S. F. Schlossman, *Blood* **53**, 1066 (1979).
11. A. B. Cosini, H. H. Wortis, F. L. Delmonico, P. S. Russell, *Surgery* **80**, 155 (1976); R. L. Edelson *et al.*, *Cancer Chemother. Rep.* **63**, 675 (1979).
12. D. H. Margulies, W. M. Kuel, M. D. Scharff, *Cell* **8**, 405 (1976).
13. We thank M. D. Scharff (Albert Einstein College of Medicine) for providing the P3 × 63Ag8U$_1$ myeloma cell line for cell fusion; A. Penta, C. O'Brien, J. McDowell, K. Singer, M. A. Talle, and M. DeMaria for technical assistance; and L. M. Grappi and C. Brain for secretarial assistance. The research was supported in part by NIH training grant CA 09172 and NIH grants AI 12069, AI 19589, and CA 06516.

7 May 1979; revised 20 June 1979

Ciliary Membrane Alterations Occurring in Experimental *Mycoplasma pneumoniae* Infection

Abstract. *Experimental infection of hamster ciliated tracheal epithelium in organ culture with virulent* Mycoplasma pneumoniae *resulted in the deterioration of ciliary necklaces and an altered distribution of membrane-associated particles on the shafts of the affected cilia. To our knowledge this is the first report of an altered disposition of ciliary membrane-associated particles in response to a specific infectious agent.*

Infections due to *Mycoplasma pneumoniae* are a major cause of respiratory disease in children and young adults (*1*). The general clinical spectrum of the disease ranges from upper respiratory tract infections, bronchitis, and tracheitis to primary atypical pneumonia (*1*). The disease is self-limiting and rarely fatal (*2*).

Investigations of the cellular basis of experimental and natural *M. pneumoniae* disease (*2–4*) have revealed ciliostasis and degenerating abnormal epithelial cells. Ultrastructural and biochemical studies also have demonstrated that in order to be fully pathogenic the organism must be specifically oriented to the host cell epithelial surface by means of a specialized terminal organelle (*4*). With the use of the freeze-etch technique, a new facet of the pathogenesis of experimental *M. pneumoniae* disease has been revealed. In these experiments, freeze-etching of hamster tracheal epithelium after incubation in organ culture with virulent *M. pneumoniae* demonstrated marked configurational alterations of the membrane-associated particles of the cilia (*5*).

Inspection of the freeze-etch replicas showed that control epithelial cells maintained in organ culture up to 48 hours retained ultrastructural integrity with their in vivo correlates (Fig. 1, A and B). A particularly prominent feature revealed by freeze-etching was the ciliary necklace, a complex of membrane-associated particles at the base of each cilium (*6*). The ciliary necklaces of epithelial cell cilia from tracheae fixed immediately after resection were comprised of generally five rows of evenly spaced particles at the base of each cilium which extended up the shaft a distance of approximately 0.2 μm (Fig. 1A). Other membrane-associated particles appeared scattered randomly and uniformly over the fractured surfaces of the cilia (Fig. 1A). This configuration of ciliary necklace and membrane-associated particles was reliably retained with minimum variability in control organ culture specimens for up to 48 hours (Fig. 1B). The membrane-associated particles of the ciliary necklaces and on the shafts of the cilia measured approximately 100 Å in diameter in both freshly fixed and organ culture specimens.

Replicas from the experimentally infected specimens showed that the highly organized ciliary necklaces were severely altered within the first 24 hours. In some cases, roughly organized remnants of the necklaces were observed; however, the general view of this area illustrated the complete disarray of the necklace particles and, in many cases, the ciliary necklace was completely absent (Fig. 1C). Membrane-associated particles observed over the ciliary shaft in infected specimens also measured approximately 100 Å in diameter and appeared clumped and unevenly distributed.

Our studies have indicated that a relatively heavy inoculum of the pathogen is necessary to produce disorganization and decreased frequency of ciliary beat in vitro. In the infected tissues, *M. pneumoniae* is observed frequently inter-

0036-8075/79/1019-0349$00.50/0

spersed among the cilia and specifically oriented to the host cell surface (Fig. 1C). From these studies it is not clear whether direct contact of organism and cilium is required for membrane alteration or injury (or both), or whether the effect is secondary to more general damage to the epithelial cells.

Our studies reflect an important in vitro correlate of natural *M. pneumoniae* disease. The ciliary necklace is thought to function in concert with the 9 + 2 microtubular doublets of the cilium (an arrangement of nine peripheral pairs and two central pairs of ciliary microtubules visible by electron microscopy when the cilium is viewed in cross section) as a membrane-microtubule complex (*6*). It has been suggested that the necklace may function much as a timing device for the ciliary beat by regulating localized membrane permeability (*6*). The disruption of the ciliary necklace observed in infected epithelium may represent the basis for in vitro ciliostasis. In natural disease the diminished ability of cilia to clear the pathogen as well as secretions from the respiratory tract during infection may provide an optimal environment for increased colonization by this pathogen during the course of the disease. Ciliary dysfunction may also relate to the clinical feature of prolonged paroxysmal cough and to the pathologic finding of segmental or subsegmental atelectasis in the lung.

To our knowledge these findings comprise the first report of the altered disposition of ciliary membrane-associated particles in response to a specific infectious agent. Such alterations may reflect critical changes in the structure, position, and function of integral membrane proteins of the cilia. The freeze-etch technique employed for these studies has provided an additional perspective to the study of infectious disease pathogenesis at the molecular level.

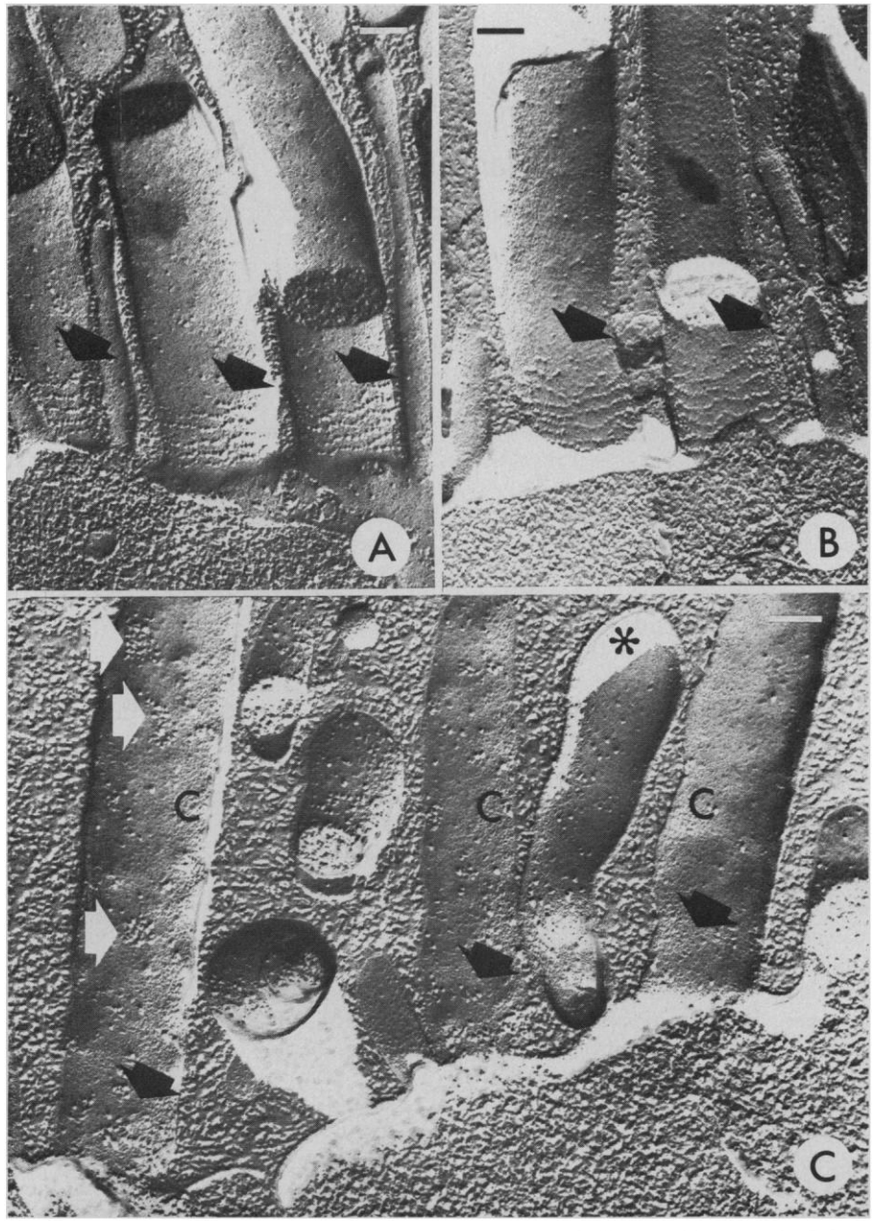

Fig. 1. (A) Electron micrograph demonstrating the structure of ciliary necklaces on the P-fracture face of hamster tracheal epithelium fixed immediately upon resection (arrows). The necklace is comprised of four to six, generally five, evenly spaced strands of membrane-associated particles at the base of each cilium. Note also the uniform distribution of particles on the shafts of the cilia. Bar equals 100 nm. (B) Electron micrograph illustrating the retention of the ciliary necklaces of epithelial cell cilia that may be observed after 24 hours of incubation in tracheal organ culture (arrows). Bar equals 100 nm. (C) Freeze-etch preparation of tracheal epithelial cells incubated in organ culture for 24 hours with virulent *Mycoplasma pneumoniae*. A mycoplasma cell indicated by an asterisk (*) is seen between two cilia (*C*). Black arrows at the bases of the cilia indicate areas of disrupted and absent ciliary necklaces in both E- and P-fracture faces. White arrows indicate areas of clumping of membrane-associated particles on the ciliary shaft. Bar equals 100 nm.

JOHNNY L. CARSON
ALBERT M. COLLIER
WALLACE A. CLYDE, JR.
Infectious Disease Division, Department of Pediatrics, and *Frank Porter Graham Child Development Center, University of North Carolina, Chapel Hill 27514*

References and Notes

1. F. W. Denny, W. A. Clyde, Jr., W. Paul Glezen, *J. Infect. Dis.* **123**, 74 (1971).
2. A. M. Collier and W. A. Clyde, Jr., *Am. Rev. Respir. Dis.* **110**, 765 (1974).
3. D. A. Powell, P. C. Hu, M. Wilson, A. M. Collier, J. B. Baseman, *Infect. Immun.* **13**, 959 (1976).
4. M. H. Wilson and A. M. Collier, *J. Bacteriol.* **125**, 332 (1976).
5. The experiments were performed by preparing hamster tracheal organ cultures in a manner similar to that described by Collier *et al.* (*7*). Experimental cultures were inoculated with 2.5×10^8 colony-forming units of *Mycoplasma pneumoniae* M129B16 per milliliter in Hayflick broth medium (*8*). Control and experimental tracheal organ cultures were incubated in Hayflick broth medium for 24 and 48 hours at 37°C in air with 5 percent CO_2. After incubation, the organ cultures were fixed in a solution of 2 percent glutaraldehyde and 2 percent paraformaldehyde in 0.1*M* phosphate buffer, *p*H 7.3. Some tracheae were fixed immediately after resection without incubation as organ cultures to provide in vivo correlate samples for comparison with in vitro control tissues. The epithelial layer of cells was dissected from the tracheae, rinsed overnight in phosphate buffer (*p*H 7.3), followed by a 1-hour treatment in a cryoprotectant consisting of 25 percent glycerol in 0.1*M* phosphate buffer, *p*H 7.3. The cells were frozen on gold specimen stages in liquefied Freon 22 and maintained in liquid nitrogen. Freeze-etching was carried out in a Balzers M360 instrument. The specimens were etched for 2 minutes at −100°C, shadowed with platinum and carbon, and coated with carbon. The replicas were cleaned in 5 percent sodium dichromate in 50 percent H_2SO_4, retrieved on standard copper grids, and viewed with a Zeiss

EM-10 electron microscope at an accelerating voltage of 60 kV.
6. N. B. Gilula and P. Satir, *J. Cell Biol.* **53**, 494 (1972).
7. A. M. Collier, W. A. Clyde, Jr., F. W. Denny, *Proc. Soc. Exp. Biol. Med.* **132**, 1153 (1969).
8. L. Hayflick, *Tex. Rep. Biol. Med.* **23**, 285 (1965).
9. We thank Drs. R. M. Brown, Jr., and D. W. Misch for their review of and comments on this manuscript, and S. S. Hu for technical assistance. Supported by SCOR grant HL19171 from the National Heart, Lung, and Blood Institute and training grant AI07151 from the National Institute of Allergy and Infectious Diseases.

11 June 1979; revised 6 August 1979

Neural Axis Representing Target Range in the Auditory Cortex of the Mustache Bat

Abstract. *In echolocating bats, the primary cue for determining distance to a target is the interval between an emitted orientation sound and its echo. Whereas frequency is represented by place in the bat cochlea, no anatomical location represents target range. Target range is coded by the time interval between grouped discharges of primary auditory neurons in response to both the emitted sound and its echo. In the frequency-modulated-signal processing area of the auditory cortex of the mustache bat (*Pteronotus parnellii rubiginosus*), neurons respond poorly or not at all to synthesized orientation sounds or echoes alone but respond vigorously to echoes following the emitted sound with a specific delay from targets at a specific range. These range-tuned neurons are systematically arranged along the rostrocaudal axis of the frequency-modulated-signal processing area according to the delays to which they best respond, and thus represent target range in terms of cortical organization. The frequency-modulated-signal processing area therefore shows odotopic representation.*

In the mustache bat (*Pteronotus parnellii rubiginosus*), the auditory cortex has been found to have at least three specialized areas for processing different types of biosonar information: the Doppler-shifted constant-frequency (DSCF), frequency modulated (FM), and CF/CF processing areas (Fig. 1A) (*1*-*6*). Neurons of the DSCF processing area are arranged along two axes, one representing echo amplitude (target subtended angle), the other representing echo frequency (target velocity information) (*2*). The DSCF processing area consists of two functional subdivisions adapted for target detection or localization (*3*). The FM and CF/CF areas process information carried by different combinations of information-bearing elements in the emitted biosonar signal and its echo (*4*-*6*). We report that the FM processing area represents target-range information along an anatomical axis without a corresponding anatomical dimension at the periphery.

The mustache bat emits biosonar signals (orientation sounds), each of which contains four harmonics. Each harmonic consists of a CF component and an FM component. Therefore, there are eight components (CF_{1-4}, FM_{1-4}) in each emitted signal (*1*, *5*, *7*). Echoes that elicit behavioral responses in the mustache bat always overlap with the emitted signal (inset, Fig. 1C). As a result, biosonar information must be extracted from a complex sound with up to 16 components.

Neurons in the FM processing area are maximally excited only when an echo from an orientation sound arrives after a particular delay. The essential elements in such paired stimuli are the first harmonic FM component (FM_1) in the orientation sound and one or more higher harmonic FM components (FM_{2-4}) in the echo. Therefore, these neurons are called FM_1-FM_n facilitation neurons (*4*, *5*).

One of the most important aspects of echolocation is ranging. The primary cue for ranging is the delay of the echo from the emitted sound. The FM_1-FM_n facilitation neurons are sensitive to this delay and are therefore range-sensitive. Range-sensitive neurons can be classified into two categories, tracking and range-tuned. The best delays (BD's) (*8*) of tracking neurons shorten and their delay-tuning curves become narrower as the bat changes the signal repetition rate and duration as it approaches a target. These neurons zero in on the target, rejecting echoes from more distant objects (*4*, *5*). Range-tuned neurons, on the other hand, are tuned to particular echo delays, regardless of repetition rate and duration of paired stimuli. They respond to the target only when it is within a certain narrow range (*5*). The obvious question is whether range-tuned neurons with different BD's (that is, best ranges) are systematically arranged along an axis in the FM processing area to represent target range information.

Experiments were performed with 12 mustache bats collected in Panama. The activity of single neurons was recorded in unanesthetized bats with a tungsten-wire electrode (5- to 10-μm tip) during the period from 4 days to 4 weeks after surgery to expose the skull. When necessary, local anesthetic (Xylocaine) and tranquilizer (droperidol) were administered. Acoustic stimuli were pure (CF) tones, FM sounds, and combinations of them that mimicked the biosonar signal-echo pair in the search, approach, and terminal phases of echolocation in this species (*9*). The stimuli were delivered from a loudspeaker 73 cm in front of the animal in a soundproof, echo-suppressed room. For details of the surgery and the stimulation and recording systems, see (*4*) and (*5*).

In the first stage of our experiment, we inserted an electrode orthogonal to the surface of the FM processing area and recorded single-unit activity at various depths to determine whether there was columnar organization for response parameters, such as best frequency, minimum threshold, and frequency bandwidth, with pure tones, FM sounds, and pairs of sounds used to elicit facilitation. We also measured BD, threshold at BD, and width of the delay-tuning curves with pairs of sounds eliciting the strongest facilitation. Neurons at depths between 200 and 1000 μm had nearly identical response characteristics, including BD's. (At depths less than 200 μm, the signal-to-noise ratio was usually small and responses to acoustic stimuli were poor.)

Confirmation of the columnar organization of BD's simplified our study of cortical representation of target range, because we could rely on the uniformity of activity at different depths in the cortex. To gather data from many locations in the cortical plane, we inserted the electrode at a 30° angle into the FM processing area; neuronal responses were studied at 200-μm intervals. We plotted BD's of range-tuned neurons only on a surface map of the cerebral cortex that was drawn prior to the recordings.

The FM processing area consists of three major clusters: FM_1-FM_3, FM_1-FM_4, and FM_1-FM_2 facilitation neurons (*4*), which are usually arranged dorsal to ventral in that order (Fig. 1B). For each electrode penetration through those clusters in the rostrocaudal direction, BD systematically varied. Figure 1B gives a schematic representation of the iso-BD contour lines that comprise a target-range axis. Neurons with extremely short BD's were recorded only at the

0036-8075/79/1019-0351$00.50/0